Journal of Coordination Chemistry

ISSN: 0095-8972 (Print) 1029-0389 (Online) Journal homepage: http://www.tandfonline.com/loi/gcoo20

Syntheses, crystal structures, electrochemical studies, and antioxidant activities of zinc(II) and copper(II) complexes with bis(2-benzimidazolyl) aniline derivatives

Huilu Wu, Jiawen Zhang, Yanhui Zhang, Chengyong Chen, Zhen Li, Mingchang Wu & Zaihui Yang

To cite this article: Huilu Wu, Jiawen Zhang, Yanhui Zhang, Chengyong Chen, Zhen Li, Mingchang Wu & Zaihui Yang (2015) Syntheses, crystal structures, electrochemical studies, and antioxidant activities of zinc(II) and copper(II) complexes with bis(2-benzimidazolyl) aniline derivatives, Journal of Coordination Chemistry, 68:5, 835-847, DOI: 10.1080/00958972.2014.1003549

To link to this article: http://dx.doi.org/10.1080/00958972.2014.1003549

Journal of Coordination Chemistry, 2015
Vol. 68, No. 5, 835–847, http://dx.doi.org/10.1080/00958972.2014.1003549

Syntheses, crystal structures, electrochemical studies, and antioxidant activities of zinc(II) and copper(II) complexes with bis(2-benzimidazolyl) aniline derivatives

HUILU WU*, JIAWEN ZHANG, YANHUI ZHANG, CHENGYONG CHEN, ZHEN LI, MINGCHANG WU and ZAIHUI YANG

School of Chemical and Biological Engineering, Lanzhou Jiaotong University, Lanzhou, PR China

(*Received 29 July 2014; accepted 11 December 2014*)

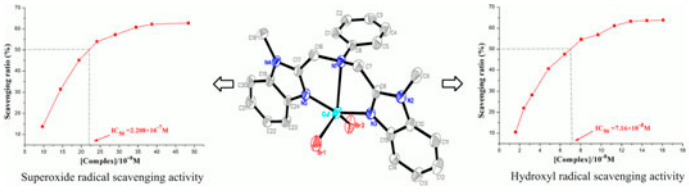

Two ligands, bis(benzimidazol-2-ylmethyl) aniline (bba) and bis(*N*-methyl-benzimidazol-2-ylmethyl) aniline (Mebba), and their transition metal complexes $[Zn(bba)(Br)_2]\cdot 2DMF$ (**1**) and $[Cu(Mebba)(Br)_2]\cdot 2DMF$ (**2**) have been synthesized and characterized by elemental analyses, molar conductivities, UV–vis spectra, IR spectra, NMR spectroscopy, and X-ray crystallography. The structure around Zn(II) can be described as distorted tetrahedral. Complex **2** can be described as distorted trigonal bipyramidal. Cyclic voltammograms of **2** indicate a quasireversible Cu^{2+}/Cu^{+} couple. Additionally, the antioxidant activities of the free ligands and their complexes were determined by the superoxide and hydroxyl radical scavenging methods *in vitro*. Complexes **1** and **2** possess potent hydroxyl radical scavenging activity and better than standard antioxidants such as vitamin C and mannitol. Complex **2** possesses excellent superoxide radical activity.

Keywords: Benzimidazole; Metal complex; Crystal structure; Electrochemistry; Antioxidation

1. Introduction

The structural, spectroscopic, and electronic properties of metal centers present in biological systems are crucial to understand their role in nature [1, 2]. These centers are often modeled using small molecules containing donors that reproduce the coordination around the metal ion [3–5]. In particular, utilization of highly symmetrical multitopic ligands with N donors to construct supramolecular structures is of high interest [6]. Among them, rigid ligands are often employed in a designed strategy to construct coordination complexes with predictable

*Corresponding author. Email: wuhl@mail.lzjtu.cn

topologies [7, 8], while flexible ligands with additional functional groups can adopt more conformations and coordination modes according to the geometric requirements of different metal ions, which may lead to more intriguing topologies and properties [9].

Since the benzimidazole unit is a building block for a variety of compounds which have crucial roles in functions of biologically important molecules, there is interest for synthesis and biological studies of benzimidazole derivatives [10, 11]. Benzimidazoles and their derivatives exhibit various biological activities as pharmaceuticals such as antitumor [12], antiviral [13], anticancer [14], antimicrobial [15], antiprotozoal [16], and anti-inflammatory or analgesic agents [17]. In our previous work [18, 19], we investigated the coordinating ability of some benzimidazole ligands and their complexes [20, 21]. The syntheses, crystal structures, electrochemical properties, and antioxidant activities of zinc(II) and copper(II) complexes are presented. The antioxidant activities (scavenging effects on $O_2^{-\cdot}$ and $OH^{-\cdot}$) of the ligands and their complexes have also been studied. Information obtained from this study will be helpful to develop some new antioxidants.

2. Experimental

2.1. *Materials and methods*

All chemicals and solvents were reagent grade and used without purification. The C, H, and N elemental analyses were determined using a Carlo Erba 1106 elemental analyzer. IR spectra were recorded from 4000 to 400 cm^{-1} with a Nicolet FT-VERTEX 70 spectrometer using KBr pellets. Electronic spectra were taken on a Lab-Tech UV Bluestar spectrophotometer. The absorbance was measured with a Spectrumlab 722sp spectrophotometer at room temperature. ^1H NMR and ^{13}C NMR spectra were obtained with a Mercury plus 400 MHz NMR spectrometer with TMS as internal standard and DMSO-d_6 as the solvent. Electrolytic conductance measurements were made with a DDS-307 type conductivity bridge using 3×10^{-3} M solutions in DMF at room temperature. Electrochemical measurements were performed on a LK2005A electrochemical analyser under nitrogen at 283 K. A glassy carbon working electrode, a platinum wire auxiliary electrode and a Ag/AgCl reference electrode ($[Cl^-] = 1.0$ M L^{-1}) were used in the three-electrode measurements. The electroactive component was at 1.0×10^{-3} M dm^{-3} concentration with tetrabutylammonium perchlorate (0.1 M dm^{-3}) used as the supporting electrolyte in DMF. The synthetic route of Mebba is shown in scheme 1.

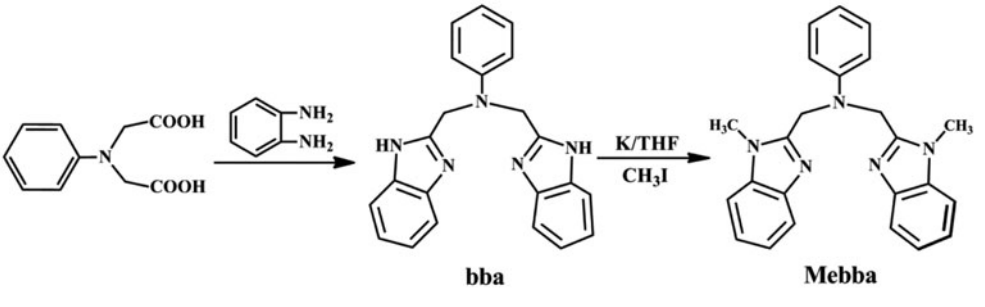

Scheme 1. Synthesis of ligands bba and Mebba.

2.2. *Preparation of the ligand and its complex*

2.2.1. Synthesis of bis(benzimidazol-2-ylmethyl) aniline (bba). The ligand bba was synthesized according to the procedure reported [19, 22]. Yield: 75.8%, m.p.: 258–259 °C. Elemental analysis for $C_{22}H_{19}N_5$: calculated (%): C, 74.77; H, 5.42; N, 19.82. Found (%): C, 74.79; H, 5.31; N, 19.93. IR (KBr; ν/cm^{-1}): 744 ν(o–Ar), 1298 ν(C–N), 1445 ν(C=N), 1610 ν(C=C). ^{1}H NMR (400 MHz, d^6-DMSO): δ = 7.196–7.681(m, 10H, benzimidazole), 6.551–7.100(m, 5H, Ph), 5.140(s, 4H CH_2). UV–visible (in DMF), λ_{max} (nm): 277 and 282. Molar conductance: Λ_M (DMF solution, 297 K): 2.69 S cm^{2}M^{-1}.

2.2.2. Synthesis of bis(*N*-methylbenzimidazol-2-ylmethyl) aniline (Mebba). 5.3 g (0.015 M) bis(benzimidazol-2-ylmethyl) aniline (bba) with 1.17 g (0.03 M) potassium in 150 mL dried tetrahydrofuran was followed by adding 4.26 g (0.03 M) iodomethane. The resulting solution was concentrated and recrystallized from methanol giving pale yellow block crystals of Mebba. Yield : 62%, m.p.: 236–238 °C. Elemental analysis for $C_{24}H_{23}N_5$: calculated (%): C, 75.56; H, 6.08; N, 18.36. Found (%): C, 75.43; H, 6.17; N, 18.31. IR (KBr; ν/cm^{-1}): 744 ν(o–Ar), 1278 ν(C–N), 1467 ν(C=N), 1604 ν(C=C). ^{1}H NMR (400 MHz, d^6-DMSO): δ = 7.128–7.599(m, 8H, benzimidazole), 6.639–7.093(m, 5H, Ph), 5.019(s, 4H, CH_2), 3.780(s, 6H, CH_3). UV–visible (in DMF), λ_{max} (nm): 280 and 286.

2.2.3. Preparation of complexes. To a stirred solution of bba (176.7 mg, 0.50 mmol) in hot EtOH (10 mL) was added to a solution of $ZnBr_2$ (112.6 mg, 0.50 mmol) in EtOH (10 mL). A white crystalline product formed rapidly. The precipitate was filtered off, washed with EtOH and absolute Et_2O, and dried *in vacuo*. The dried precipitate was dissolved in DMF to form a yellow solution into which Et_2O was allowed to diffuse at room temperature. Crystals suitable for X-ray measurement were obtained after several days. Complex **2** was prepared by a similar procedure as for **1**.

1, Yield: 75%. Elemental analysis for $C_{28}H_{33}ZnBr_2N_7O_2$: calculated (%): C, 59.52; H, 5.89; N, 17.35. Found (%): C, 59.48; H, 5.91; N, 17.36. IR (KBr; ν/cm^{-1}): 752 ν (*o*–Ar), 1276 ν(C–N), 1447 ν(C=N), 1597 ν(C=C). ^{1}H NMR (400 MHz, d^6-DMSO): δ = 7.351–7.910(m, 8H, benzimidazole), 6.651–7.117(m, 5H, Ph), 5.073(s, 4H, CH_2). ^{13}C NMR (DMSO-d_6, 400 MHz): δ (ppm) 153.8, 147.2, 129.1, 122.8, 119.3, 113.4, 50.1. UV–visible (in DMF), λ_{max} (nm) [ε_{max} (L M^{-1} cm^{-1})]: 275(1.72 × 10^4), 282(1.46 × 10^4). Molar conductance: Λ_M (DMF solution): 13.6 S cm^2 M^{-1}.

2, Yield: 67%. Elemental analysis for $C_{30}H_{37}CuBr_2N_7O_2$: calculated (%): C, 60.95; H, 6.31; N, 16.58. Found (%): C, 60.89; H, 6.23; N, 16.55. IR (KBr; ν/cm^{-1}): 754 ν (*o*–Ar), 1293 ν(C–N), 1454 ν(C=N), 1614 ν(C=C). UV–visible (in DMF), λ_{max} (nm) [ε_{max} (L M^{-1} cm^{-1})]: 279(1.65 × 10^4), 285(1.57 × 10^4), 750(241). Molar conductance: Λ_M (DMF solution): 26.4 S cm^2 M^{-1}.

2.3. *Antioxidant activities*

2.3.1. Hydroxyl radical scavenging activity. Hydroxyl radicals were generated in aqueous media through the Fenton-type reaction [23, 24]. The reaction mixture (3 mL) contained 1.0 mL of 0.10 mM aqueous safranin, 1 mL of 1.0 mM aqueous EDTA–Fe(II), 1 mL

of 3% aqueous H_2O_2, and a series of quantitative microadditions of solutions of the test compound. A sample without the tested compound was used as the control. The reaction mixtures were incubated at 37 °C for 30 min in a water bath. The absorbance was then measured at 520 nm. All the tests were run in triplicate and are expressed as the mean and standard deviation (SD). The scavenging effect for $OH^{-\cdot}$ was calculated from the following expression:

$$\text{Scavenging effect } (\%) = (A_{\text{sample}} - A_{\text{blank}})/(A_{\text{control}} - A_{\text{blank}}) \times 100$$

where A_{sample} is the absorbance of the sample in the presence of the tested compound, A_{blank} is the absorbance of the blank in the absence of the tested compound, and A_{control} is the absorbance in the absence of the tested compound and EDTA–Fe(II) [25].

2.3.2. Superoxide radical scavenging activity. A nonenzymatic system containing 1 mL 9.9×10^{-6} M $VitB_2$, 1 mL 1.38×10^{-4} M NBT and 1 mL 0.03 M MET was used to produce the superoxide anion ($O_2^{-\cdot}$) and the scavenging rate of $O_2^{-\cdot}$ under the influence of 0.1–1.0 μM of the test compound was determined by monitoring the reduction in rate of transformation of NBT to monoformazan dye [26]. The solutions of MET, $VitB_2$, and NBT were prepared with 0.02 M phosphate buffer (pH 7.8) avoiding light. The reactions were monitored at 560 nm with a UV/vis spectrophotometer and the rate of absorption change was determined. The percentage inhibition of NBT reduction was calculated using the equation [27]:

$$\text{percentage inhibition of NBT reduction} = (1 - k'/k) \times 100$$

where k' and k are the slopes of the straight line of absorbance values as a function of time in the presence and the absence of SOD mimic compound (SOD is superoxide dismutase), respectively. The IC_{50} values for the complexes were determined by plotting the graph of percentage inhibition of NBT reduction against the increase in the concentration of the complex. The concentration of the complex which causes 50% inhibition of NBT reduction is reported as IC_{50}.

2.4. *X-ray crystallography*

Structure diffraction intensities for **1** and **2** were collected on a Bruker Smart CCD diffractometer with graphite-monochromated Mo-K_α radiation ($\lambda = 0.71073$ Å) at 296(2) K. Data reduction and cell refinement were performed using SMART and SAINT. The structures were solved by direct methods and refined by full-matrix least squares against F^2 of data using SHELXTL software [28–30]. All hydrogens attached to carbons except for DMF groups were fixed geometrically and treated as riding with C–H = 0.93 or 0.97 Å with $U_{\text{iso}}(H) = 1.2U_{\text{eq}}(C)$. All hydrogens attached to N were fixed geometrically and treated as riding with N–H = 0.86 Å with $U_{\text{iso}}(H) = 1.2U_{\text{eq}}(N)$. Basic crystal data, description of the diffraction experiment, and details of the structure refinement are given in table 1. Selected bond distances and angles are presented in table 2.

Table 1. Crystal and structure refinement data for **1** and **2**.

Complex	**1**	**2**
Molecular formula	$C_{28}H_{33}ZnBr_2N_7O_2$	$C_{30}H_{37}CuBr_2N_7O_2$
Molecular weight	724.80	751.03
Crystal system	Triclinic	Triclinic
Space group	*P-1*	*P-1*
a (Å)	8.998(3)	11.234(3)
b (Å)	11.696(4)	12.024(3)
c (Å)	14.760(5)	12.807(4)
β (º)	91.459(4)	86.607(4)
V (Å^3)	1531.3(9)	1691.1(8)
Z	2	2
D (calculated) (g cm^{-3})	1.572	1.475
F (0 0 0)	732	762
Crystal size (mm)	0.40 × 0.38 × 0.30	0.40 × 0.38 × 0.30
θ range for data collection	1.77–24.15	1.62–25.50
h/k/l (max, min)	−9,10/ −13,13/ −16,16	−13,13/ −14,14/ −15,15
Reflections collected	9070	11,478
Independent reflections	4788/0.0599	6121/0.0622
Refinement method	Full-matrix least squares on F^2	Full-matrix least squares on F^2
Data/restraints/parameters	4788/0/366	6121/0/385
Goodness-of-fit on F^2	1.044	1.015
Final R_1, wR_2 indices [$I > 2\sigma(I)$]	0.0696/0.1841	0.0551/0.1431
R_1, wR_2 indices (all data)	0.0899/0.2120	0.1013/0.1739
Largest diff. peak and hole (e Å^{-3})	0.830/−1.300	0.795/−0.690

3. Results and discussion

The synthetic route to Mebba is shown in scheme 1. Complex **1** was prepared by reaction of bba with $ZnBr_2$ in ethanol, and **2** was prepared by a similar procedure as for **1**. All compounds are stable in atmospheric conditions. They are soluble in polar aprotic solvents such as DMF, DMSO, and CH_3CN, slightly soluble in ethanol, ethyl acetate, and chloroform, and insoluble in water, diethyl ether, and petroleum ether. The elemental analyses show their different compositions. The molar conductivities in DMF indicate that **1** and **2** are nonelectrolytes.

Table 2. Selected bond distances (Å) and angles (°) for **1** and **2**.

1			
Zn(1)–N(5)	2.016(6)	Zn(1)–N(3)	2.028(5)
Zn(1)–Br(2)	2.4104(14)	Zn(1)–Br(1)	2.4379(12)
N(5)–Zn(1)–N(3)	126.3(2)	N(5)–Zn(1)–Br(2)	105.27(17)
N(3)–Zn(1)–Br(2)	106.91(17)	N(5)–Zn(1)–Br(1)	103.36(16)
N(3)–Zn(1)–Br(1)	102.10(15)	Br(2)–Zn(1)–Br(1)	112.98(5)
N(5)–Zn(1)–N(1)	64.45(19)	N(3)–Zn(1)–N(1)	64.03(19)
Br(2)–Zn(1)–N(1)	111.93(11)	Br(1)–Zn(1)–N(1)	135.08(11)
2			
Cu(1)–N(3)	1.962(4)	Cu(1)–N(5)	1.972(4)
Cu(1)–Br(2)	2.3962(12)	Cu(1)–Br(1)	2.4713(11)
Cu(1)–N(1)	2.486(4)		
N(3)–Cu(1)–N(5)	152.93(18)	N(3)–Cu(1)–Br(2)	98.36(13)
N(5)–Cu(1)–Br(2)	98.55(13)	N(3)–Cu(1)–Br(1)	91.75(14)
N(5)–Cu(1)–Br(1)	92.47(14)	Br(2)–Cu(1)–Br(1)	132.02(4)
N(3)–Cu(1)–N(1)	76.59(16)	N(5)–Cu(1)–N(1)	76.50(16)
Br(2)–Cu(1)–N(1)	122.76(12)	Br(1)–Cu(1)–N(1)	105.22(12)

3.1. *IR, UV–visible and NMR spectra*

The IR spectral data for the compounds along with their relative assignments are given in table 3. A strong band is found at 1275 cm^{-1} along with another less strong band around 1450 cm^{-1} in the ligands. By analogy with the assigned bands of imidazole, the former is attributed to ν(C–N), while the other one is ν(C=N) [31, 32]. One shifts around 20 cm^{-1} and the other around 10 cm^{-1} in the complexes, which implies direct coordination of all two imine nitrogens to metal ions. These are the preferred nitrogens for coordination, as found in other metal complexes with benzimidazoles [33, 34]. The results agree with those determined by X-ray diffraction.

DMF solutions of bba, Mebba, and their complexes show, as expected, almost identical UV spectra. The UV bands of bba (277, 282 nm) and Mebba (280, 286 nm) are only marginally blue-shifted (2–5 nm) in their complexes, which is evidence of C=N coordination to the metal. These bands are assigned to $n \rightarrow \pi^*$ and $\pi \rightarrow \pi^*$ (imidazole) transitions. The copper(II) complex exhibits one absorption, which is assigned to a d → d transition [35].

In **1**, proton signals of benzimidazole were upfield shifted compared with free bba, indicating that these signals are attributable to coordination species existing in solution due to an inductive effect of metal ions upon complexation. Due to single-electron effects of copper in **2**, few strong signals appeared for ^{1}H NMR spectra of **2**. ^{1}H NMR and ^{13}C NMR spectra of complexes are presented in supplementary material.

3.2. *Description of the structure*

3.2.1. Crystal structure of 1. The ORTEP representation of the structure of **1**, including atom numbering scheme, is shown in figure 1, and the selected bond lengths and angles are listed in table 2. The metal is coordinated with an N_2Br_2 ligand set of which two N atoms (N(3), N(5)) are from bba and the other two bromides (Br(1), Br(2)). The coordination geometry of zinc may be best described as distorted tetrahedral. Three bonds, Zn(1)–N(3), Zn(1)–N(5), and Zn(1)–Br(2), are formed in the pyramidal plane; the distances are 2.016 (6)–2.4104(14) Å. The bond distance between Zn(1) and the apical Br(1) is 2.4379(12) Å, and the bond distances between the Zn and the basal atoms are Zn(1)–N(3) = 2.028(5) Å, Zn(1)–N(5) = 2.016(6) Å, and Zn(1)–Br(2) = 2.4104(14) Å. So the environment of the Zn(II) ion may be treated as a distorted tetrahedron. Owing to this coordination geometry, an eight-membered (ZnNNNCCC) chelating ring was constructed, connected through the Zn(II) center and displaying an 8-shaped geometry [36].

As shown in figure 2, weak supramolecular $\pi\cdots\pi$ and C–H···O, strong C–H···Br hydrogen-bonding interactions play important roles in the crystal packing modes in the complex. The planes of two benzene rings form $\pi\cdots\pi$ stacking interactions (centroid-to-centroid

Table 3. IR bonds (cm^{-1}) of compounds.

Compound	$\nu_{(Ar)}$	$\nu_{(C–N)}$	$\nu_{(C=N)}$	$\nu_{(C=C)}$
bba	744	1298	1445	1610
1	752	1276	1447	1597
Mebba	744	1278	1467	1604
2	754	1293	1454	1614

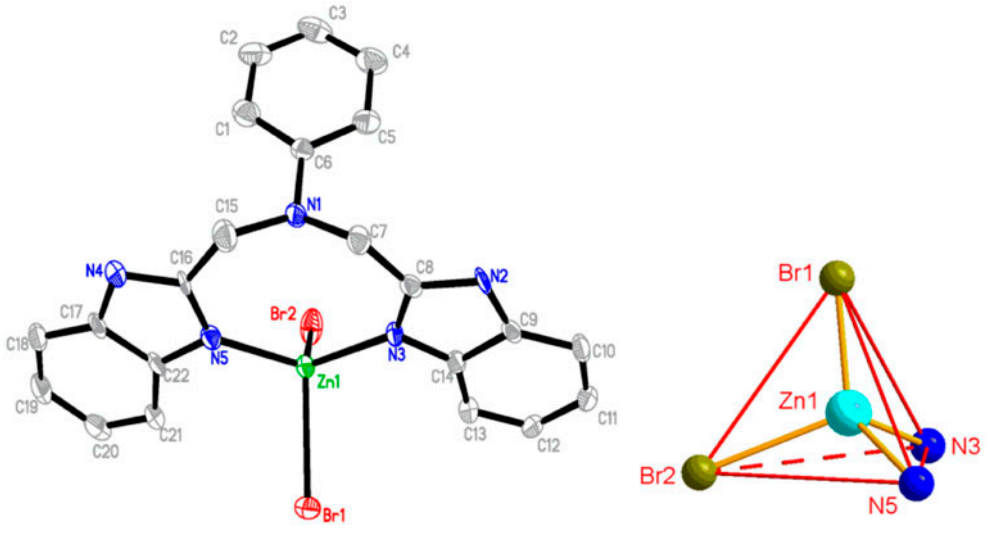

Figure 1. Molecular structure and atom numbering of $[Zn(bba)]Br_2$ with hydrogens omitted for clarity.

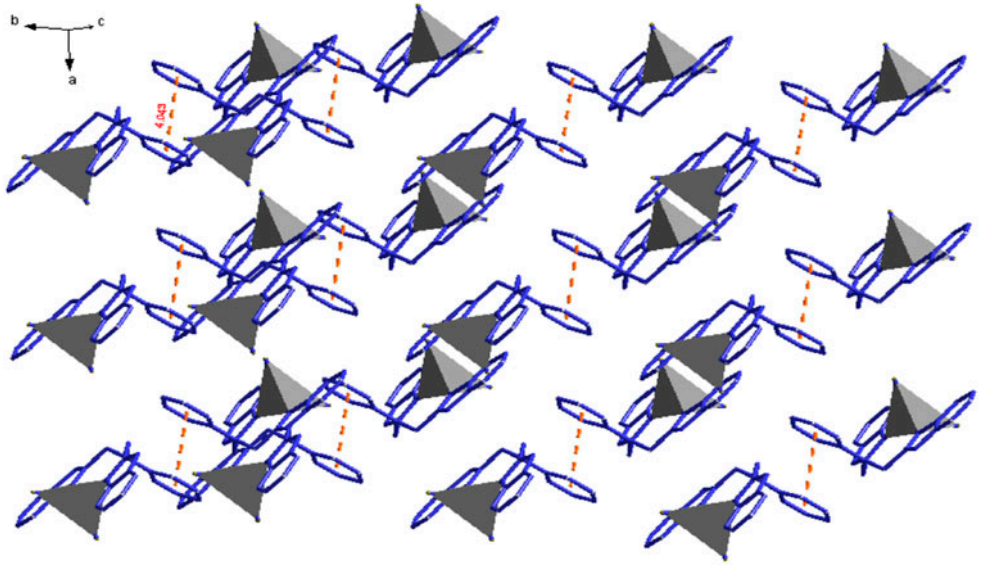

Figure 2. The $\pi\cdots\pi$ interactions and packing modes in **1** (hydrogens are omitted).

distances: 4.043 Å) along the crystallographic *a* axis. Such arrangement can make the crystal structure more stable.

3.2.2. Crystal structure of 2. Complex **2** crystallized in the triclinic space group *P-1* (figure 3). The asymmetric unit consists of a $[Cu(Mebba)]^{2+}$, two bromides, and 2 DMF

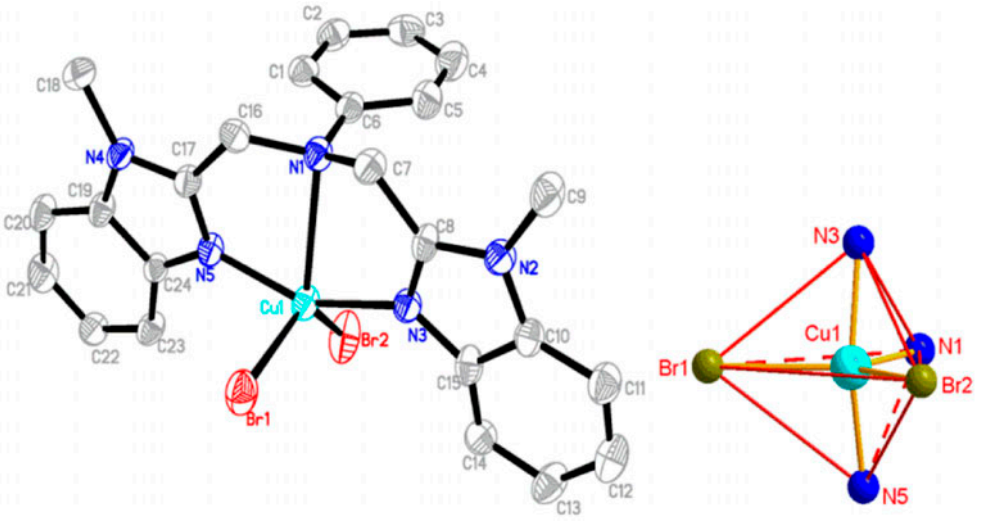

Figure 3. Molecular structure of **2** with hydrogens omitted for clarity.

molecules. The Cu(II) is five-coordinate with a CuN_3Br_2 coordination environment. The Mebba ligand is a terdentate N-donor and two bromides of a monodentate salicylate complete the coordination. The coordination of the Cu(II) may be best described as distorted trigonal bipyramidal ($\tau_1 = 0.5$), with approximate $C3$ symmetry. The parameter τ is defined as $(\beta - \alpha)/60$ [where β = N(3)–Cu(1)–N(5) and α = Br(2)–Cu(1)–Br(1)], and its value varies from 0 (in regular square-based pyramidal) to 1 (in regular trigonal bipyramidal) [37]. The axial sites are occupied by N(3) and N(5), with Cu(1)–N(3) = 1.962(4) Å, Cu(1)–N(5) = 1.972(4) Å, and N(3)–Cu(1)–N(5) = 152.93(18)°. The trigonal plane is occupied by ligating N atoms of the benzimidazolyl groups and two bromides, N(1)/Br(1)/Br(2). The angles of Br(1)–Cu(1)–N(1), Br(2)–Cu(1)–N(1), and Br(2)–Cu(1)–Br(1) are 105.22(12)°, 122.76(12)°, and 132.02(4)°, respectively. The N(3)–Cu(1)–N(1) = 76.59(16)°, N(3)–Cu(1)–Br(1) = 91.75(14)°, and N(3)–Cu(1)–Br(2) = 98.36(13)° angles appear essentially imposed by the stereochemistry of the ligand Mebba and bromide.

As shown in figure 4, weak C–H···Br and strong C–H···O hydrogen-bonding interactions play important roles in the crystal packing modes in **2**. Neighboring chains are connected by C–H···Br hydrogen bonds (C–Br 3.750–4.119 Å) and C–H···O hydrogen bonds (C–O 3.295–3.331 Å), generating an infinite 2-D layer.

From the crystal structures of **1** and **2**, their structural conformations are mainly controlled by the ligands and metal centers, and also influenced by the coordination capabilities of counter anions. The intramolecular weak interactions also help to assemble the crystal structures into different dimensions.

3.3. *Electrochemical studies*

The electrochemical properties of **2** were studied by cyclic voltammetry (CV) in DMF. The data are collected in table 4, and a voltammogram is shown in figure 5. The Cu(II) complex exhibits a pair of cathodic and anodic waves. The separation between the cathodic and

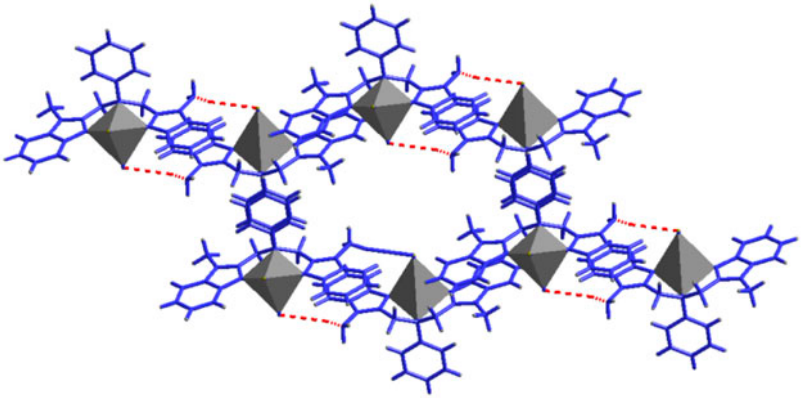

Figure 4. 3-D layer formed via weak C–H···Br hydrogen-bonding interactions in **2**.

Table 4. Electrochemical data of **2**.

Complex	E_{pc}	E_{pa}	ΔE_p	$E_{1/2}$	i_{pa}	i_{pc}	I
2	0.2756	0.3865	0.1109	0.3311	4.56	4.82	0.946

$\Delta E = E_{pa} - E_{pc}$; $E_{1/2} = (E_{pa} + E_{pc})/2$; $I = i_{pa}/i_{pc}$.

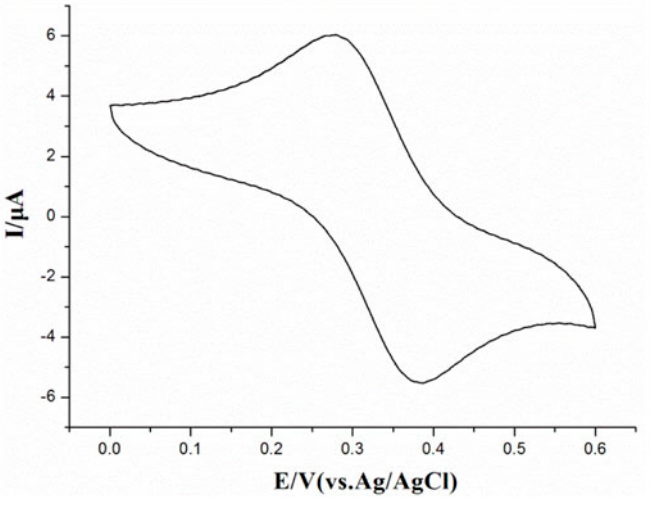

Figure 5. Cyclic voltammogram of **2** recorded with a platinum electrode in DMF solution containing $(n\text{Bu})_4\text{N}\cdot\text{ClO}_4$ (0.1 M) (scan rate = 0.05 V S^{-1}).

anodic peak potentials ΔE_p ($\Delta E_{pa} - E_{pc}$) and the current I (i_{pa}/i_{pc}) indicates a quasireversible redox process assignable to the Cu(II)/Cu(I) couple [38]. The neutral uncomplexed Mebba is not electroactive over the range −1.3 to +1.3 V. According to previous reports [39], a

transition metal complex must have a redox potential below 0.65 V [$E°(O_2–O_2^-)$] and above −0.33 V [$E°(O_2–O_2^-)$] such that catalysis can be an effective mimic of superoxide dismutase but toxic single oxygen cannot be formed; so the redox potential 0.1109 V shows that **2** may have SOD activity.

3.4. *Antioxidant activities*

Generation of reactive oxygen species (ROS) is a normal process in the life of aerobic organisms. $OH^{-\cdot}$ and $O_2^{-\cdot}$ are two clinically important ROS in the human body [40]. They are produced in most organ systems and participate in various physiological and pathophysiological processes such as carcinogenesis, aging, viral infection, inflammation, and others [41]. Consequently, in this study, the ligands bba, Mebba, and their complexes are studied for their antioxidant activity by comparing their scavenging effects on $OH^{-\cdot}$ and $O_2^{-\cdot}$.

3.4.1. Hydroxyl radical scavenging activity. We compared the abilities of the present compounds to scavenge hydroxyl radicals with those of the well-known natural antioxidants such as mannitol and vitamin C, using the same method as reported in previous studies [42–44]. The 50% inhibitory concentration (IC_{50}) value of mannitol and vitamin C are 9.6×10^{-3} and 8.7×10^{-3} M, respectively. Figure 6 shows the plots of hydroxyl radical scavenging effect (%) for **1** and **2**; the IC_{50} values of **1** and **2** are 9.02×10^{-5} and 7.16×10^{-8} M, respectively, but bba and Mebba do not have activity. The results indicate that the binding strength of the complexes follows the order **2** > **1**. The two transition metal complexes exhibit better scavenging activity than mannitol and vitamin C. The lower IC_{50} values observed in antioxidant assays demonstrate that the complexes have potential to be applied as scavengers to eliminate radicals.

3.4.2. Superoxide radical scavenging activity. As another assay of antioxidant activity and superoxide radical ($O_2^{-\cdot}$) scavenging activity has been investigated [45]. As can be seen

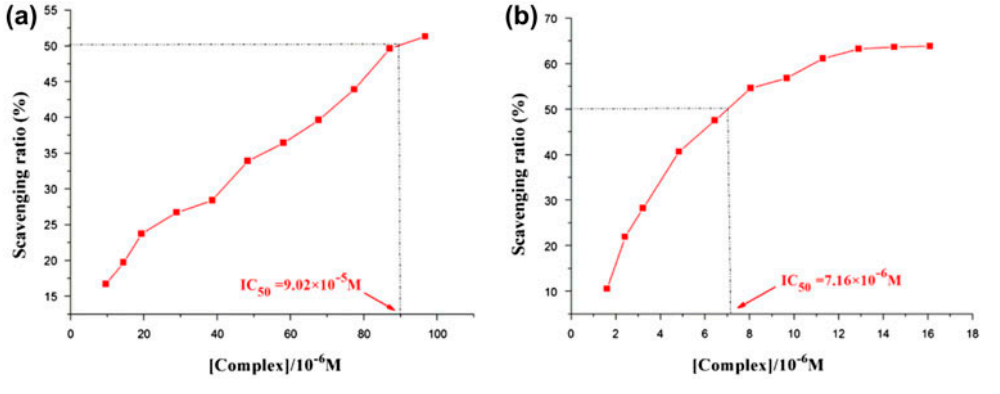

Figure 6. The inhibitory effect of **1** (a) and **2** (b) on $OH^{-\cdot}$ radicals; the suppression ratio increases with increasing concentration of the test compounds.

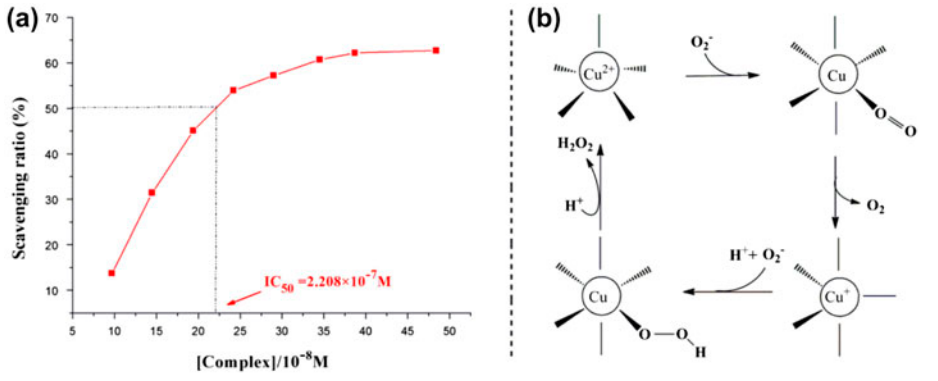

Figure 7. (a) The superoxide radical scavenging effect (%) for the Cu(II) complex. (b) Possible reaction mechanism of **2** on superoxide radical.

from figure 7(a), the IC_{50} value of **2** is 2.208×10^{-7} M. Therefore, **2** demonstrates good SOD activities with respect to the standard SOD mimic copper complex ($IC_{50} = 2.6 \times 10^{-5}$ M) [46], but **1** does not have activity. From figure 7(b), we found that this may be attributed to the reaction mechanism on superoxide radical [47, 48]. According to the mechanism of copper complex, in the first step of the reaction, the superoxide radical is oxidized by Cu(II) to molecular oxygen. Subsequently, a second superoxide anion is reduced by Cu(I) to produce hydrogen peroxide. The result indicates that **2** exhibits good superoxide radical scavenging activity and may be an inhibitor (or a drug) to scavenge superoxide radical ($O_2^{\cdot-}$) *in vivo*, but needs further investigation, which is consistent with the above electrochemical studies.

4. Conclusion

The ligands bba, Mebba, and their complexes have been synthesized and characterized. The structure and geometry of two transition metal complexes were analyzed through single crystal X-ray diffraction. The cation of **1** can be described as distorted tetrahedral. The geometric structure of **2** may be treated as distorted trigonal bipyramidal. Complexes **1** and **2** possess potent hydroxyl radical scavenging activity, better than standard antioxidants such as vitamin C and mannitol. Furthermore, **2** possesses significant superoxide radical activity. Electrochemical studies show quasireversible redox behavior for the copper(II) complex. These findings clearly indicate that metal complexes with benzimidazole have applications of antioxidants, which warrants further *in vivo* experiments and pharmacological assays.

Supplementary material

Crystallographic data for **1** and **2** have been deposited with the Cambridge Crystallographic Data Center as supplementary publication CCDC reference numbers 999911 and 999910.

Copies of the data can be obtained, free of charge, on application to the CCDC, 12 Union Road, Cambridge CB2 1EZ, UK. Tel: +44 01223 762910; Fax: +44 01223 336033; E-mail: deposit@ccdc.cam.ac.uk or http://www.ccdc.cam.ac.uk.

Funding

The present research was supported by the National Natural Science Foundation of China [grant number 21367017]; the Fundamental Research Funds for the Gansu Province Universities [grant number 212086]; Natural Science Foundation of Gansu Province [grant number 1212RJZA037]; 'Qing Lan' Talent Engineering Funds for Lanzhou Jiaotong University.

Supplemental data

Supplemental data for this article can be accessed here [http://dx.doi.org/10.1080/00958972.2014.1003549].

References

[1] N.L. Rosi, J. Kim, M. Eddaoudi, B. Chen, M. O'Keeffe, O.M. Yaghi. *J. Am. Chem. Soc.*, **127**, 1504 (2005).
[2] H. Zheng, E.Q. Gao, Z.M. Wang, C.H. Yan, M. Kurmoo. *Inorg. Chem.*, **44**, 862 (2005).
[3] J. Fan, H.F. Zhu, T. Okamura, W.Y. Sun, W.X. Tang, N. Ueyama. *Chem. Eur. J.*, **9**, 4724 (2003).
[4] S. Leininger, B. Olenyuk, P.J. Stang. *Chem. Rev.*, **100**, 853 (2000).
[5] M.V. Marinho, M.I. Yoshida, K.J. Guedes, K. Krambrock, A.J. Bortoluzzi, M. Hörner, F.C. Machado, W.M. Teles. *Inorg. Chem.*, **43**, 1539 (2004).
[6] B.F. Abrahams, S.J. Egan, R. Robson. *J. Am. Chem. Soc.*, **121**, 3535 (1999).
[7] H. Chun, D. Kim, D.N. Dybtsev, K. Kim. *Angew. Chem. Int. Ed.*, **43**, 971 (2004).
[8] X.C. Huang, Y.Y. Lin, J.P. Zhang, X.M. Chen. *Angew. Chem. Int. Ed.*, **45**, 1557 (2006).
[9] B.S. Hammes, D. Ramos-Maldonado, G.P.A. Yap, A.L. Rheingold, V.G. Young Jr., A.S. Borovik. *Coord. Chem. Rev.*, **174**, 241 (1998).
[10] J. Velík, V. Baliharová, J. Fink-Gremmels, S. Bull, J. Lamka, L. Skálová. *Res. Vet. Sci.*, **76**, 95 (2004).
[11] M. Devereux, D.O. Shea, A. Kellett, M. McCann, M. Walsh, D. Egan, C. Deegan, K. Kędziora, G. Rosair, H. Müller-Bunz. *J. Inorg. Biochem.*, **101**, 881 (2007).
[12] J. Mann, A. Baron, Y. Opoku-Boahen, E. Johansson, G. Parkinson, L.R. Kelland, S. Neidle. *J. Med. Chem.*, **44**, 138 (2001).
[13] J. Cheng, J.T. Xie, X.J. Luo. *Bioorg. Med. Chem. Lett.*, **15**, 267 (2005).
[14] A. Gellis, H. Kovacic, N. Boufatah, P. Vanelle. *Eur. J. Med. Chem.*, **43**, 1858 (2008).
[15] O.O. Guven, T. Erdogan, H. Göker, S. Yıldız. *Bioorg. Med. Chem. Lett.*, **17**, 2233 (2007).
[16] H. Torres-Gómez, E. Hernández-Núñez, I. León-Rivera, J. Guerrero-Alvarez, R. Cedillo-Rivera, R. Moo-Puc, R. Argotte-Ramos, M.C. Rodriguez-Gutierrez, M.J. Chan-Bacab, G. Navarrete-Vázquez. *Bioorg. Med. Chem. Lett.*, **18**, 3147 (2008).
[17] S.M. Sondhi, S. Rajvanshi, M. Johar, N. Bharti, A. Azam, A.K. Singh. *Eur. J. Med. Chem.*, **37**, 835 (2002).
[18] H.L. Wu, Y.H. Zhang, C.Y. Chen, J.W. Zhang, Y.C. Bai, F.R. Shi, X.L. Wang. *New J. Chem.*, **38**, 3688 (2014).
[19] H.L. Wu, B. Liu, F. Kou, F. Jia, J.K. Yuan, Y. Bai. *J. Chin. Chem. Soc.*, **59**, 836 (2012).
[20] M. Kose, M. Digrak, I. Gonul, V. Mckee. *J. Coord. Chem.*, **67**, 1746 (2014).
[21] J.A. Zhao, S.S. Li, D.D. Zhao, S.F. Chen, J.Y. Hu. *J. Coord. Chem.*, **66**, 1650 (2013).
[22] R. Cariou, J.J. Chirinos, V.C. Gibson, G. Jacobsen, A.K. Tomov, G.J.P. Britovsek, A.J.P. White. *Dalton Trans.*, **39**, 9039 (2010).
[23] S. Satyanarayana, J.C. Dabrowiak, J.B. Chaires. *Biochemistry*, **32**, 2573 (1993).
[24] C.P. Tan, J. Liu, L.M. Chen, S. Shi, L.N. Ji. *J. Inorg. Biochem.*, **102**, 1644 (2008).
[25] Z.Y. Guo, R.E. Xing, S. Liu, H.H. Yu, P.B. Wang, C.P. Li, P.C. Li. *Bioorg. Med. Chem. Lett.*, **15**, 4600 (2005).
[26] X.Y. Le, S.R. Liao, X.P. Liu, X.L. Feng. *J. Coord. Chem.*, **59**, 985 (2006).
[27] Q.H. Luo, Q. Lu, A.B. Dai, L.G. Huang. *J. Inorg. Biochem.*, **51**, 655 (1993).
[28] B.D. Wang, Z.Y. Yang, P. Crewdson, D.Q. Wang. *J. Inorg. Biochem.*, **101**, 1492 (2007).
[29] D. Suh, J.B. Chaires. *Bioorg. Med. Chem.*, **3**, 723 (1995).
[30] M. Chauhan, K. Banerjee, F. Arjmand. *Inorg. Chem.*, **46**, 3072 (2007).

[31] C.Y. Su, B.S. Kang, C.X. Du, Q.C. Yang, T.C.W. Mak. *Inorg. Chem.*, **39**, 4843 (2000).
[32] H.L. Wu, H.C. Huang, J.K. Yuan, F. Kou, G.S. Chen, B.B. Jia, Y. Yang, Y.L. Lan. *Z. Naturforsch.*, **65b**, 1334 (2010).
[33] W.K. Dong, Y.X. Sun, L. Li, S.T. Zhang, L. Wang, X.Y. Dong, X.H. Gao. *J. Coord. Chem.*, **65**, 2332 (2012).
[34] J.Y. Chen, X.X. Ren, Z.W. Mao, X.Y. Le. *J. Coord. Chem.*, **65**, 2182 (2012).
[35] H.L. Wu, J.K. Yuan, Y. Bai, G.L. Pan, H. Wang, X.B. Shu. *J. Photochem. Photobiol., B*, **107**, 65 (2012).
[36] Z.C. Liu, B.D. Wang, B. Li, Q. Wang, Z.Y. Yang, T.R. Li, Y. Li. *Eur. J. Med. Chem.*, **45**, 5353 (2010).
[37] S. Youngme, J. Phatchimkun, U. Suksangpanya, C. Pakawatchai, N. Chaichit, P. Kongsaeree, J. Krzystek, B. Murphy. *Polyhedron*, **26**, 871 (2007).
[38] W.H. Koppenol, F. Levine, T.L. Hatmaker, J. Epp, J.D. Rush. *Arch. Biochem. Biophys.*, **251**, 594 (1986).
[39] H.L. Wu, R.R. Yun, K.T. Wang, K. Li, X.C. Huang, T. Sun, Y.Y. Wang. *Z. Anorg. Allg. Chem.*, **636**, 1397 (2010).
[40] K. Tsai, T.G. Hsu, K.M. Hsu, H. Cheng, T.Y. Liu, C.F. Hsu, C.W. Kong. *Free Radical Biol. Med.*, **31**, 1465 (2001).
[41] M. Xu, Y.C. Zhang, Z.H. Xu, Z.Z. Zeng. *Inorg. Chim. Acta*, **384**, 324 (2012).
[42] S. Satyanarayana, J.C. Dabrowiak, J.B. Chaires. *Biochemistry*, **32**, 2573 (1993).
[43] H.L. Wu, J.K. Yuan, Y. Bai, G.L. Pan, H. Wang, J. Kong, X.Y. Fan, H.M. Liu. *Dalton Trans.*, **41**, 8829 (2012).
[44] Z.L. Hua, W.W. Na, W. Yuan, S. Guang. *J. Coord. Chem.*, **66**, 227 (2013).
[45] B.D. Wang, Z.Y. Yang, P. Crewdson, D.D. Wang. *J. Inorg. Biochem.*, **101**, 1492 (2007).
[46] R.N. Patel, D.K. Patel, V.P. Sondhiya, K.K. Shukla, Y. Singh, A. Kumar. *Inorg. Chim. Acta*, **405**, 209 (2013).
[47] N. Kitajima, M. Osawa, N. Tamura, Y. Morooka, T. Hirano, M. Hirobe, T. Nagano. *Inorg. Chem.*, **32**, 1879 (1993).
[48] M.D. Alessandro, M. Aschi, M. Paci, A. Di Nola, A. Amadei. *J. Phys. Chem. B*, **108**, 16255 (2004).